Journal of Molecular Spectroscopy 256 (2009) 216–227

Contents lists available at ScienceDirect

Journal of Molecular Spectroscopy

journal homepage: www.elsevier.com/locate/jms

Fourier transform emission spectroscopy and *ab initio* calculations on WO

Ram S. Ram [a,*], J. Liévin [b], Peter F. Bernath [a,c,d]

[a] Department of Chemistry, University of Arizona, Tucson, AZ 85721, USA
[b] Université Libre de Bruxelles, Service de Chimie quantique et Photophysique, CP 160/09, Av. F. D. Roosevelt 50, Bruxelles, Belgium
[c] Department of Chemistry, University of Waterloo, Waterloo, Ont., Canada N2L 3G1
[d] Department of Chemistry, University of York, Heslington, York YO10 5DD, UK

ARTICLE INFO

Article history:
Received 13 February 2009
In revised form 15 April 2009
Available online 3 May 2009

Keywords:
Emission spectroscopy
Transition metal oxide
Free radical

ABSTRACT

Emission spectra of WO have been observed in the 4000–35 000 cm^{-1} region using a Fourier transform spectrometer. Molecules were produced by exciting a mixture of WCl_6 vapor and He in a microwave discharge lamp. A $^3\Sigma^-$ state has been assigned as the ground state of WO based on a rotational analysis of the observed bands and *ab initio* calculations. After rotational analysis, a majority of strong bands have been classified into three groups. Most of the transitions belonging to the first group have an $\Omega = 0^+$ state as the lower state while the bands in the second group have an $\Omega'' = 1$ state as the lower state. These two lower states have been assigned as $X0^+$ and X1 spin components of the $X^3\Sigma^-$ ground state of WO. The third group consists of additional bands interconnected by common vibrational levels involving some very low-lying states. The spectroscopic properties of the low-lying electronic states have been predicted from *ab initio* calculations. The details of the rotational analysis are presented and an attempt has been made to explain the experimental observations in the light of the *ab initio* results.

1. Introduction

There has been considerable interest in the study of transition metal containing species due to their importance in organic and organometallic chemistry [1,2] as well as theoretical chemistry [3]. The spectroscopic studies of these molecules provide insight into chemical bonding in simple metal-containing systems. These studies are also needed to test and advance the quality of *ab initio* calculations. Because of relatively high cosmic abundances of these molecules, these species are also of astrophysical importance. In general, the electronic structure is not well understood because the complexity of the electronic spectra. The spectra of these molecules are usually complex due to presence of a large number of electronic states derived from several close-lying electronic configurations. The presence of open d-shells in transition metals gives rise to states with high spin and large orbital angular momenta. The components of high multiplicity states in these molecules are further split by substantial spin–orbit interactions which limits the validity of the usual Hund's case (a) coupling scheme. In some cases the electronic states tend towards Hund's case (c) coupling, which creates difficulty in the electronic assignments. WO is a very good example of such complexity. Although the visible bands of WO have been known for decades the electronic states remain poorly characterized.

Initial observations of WO in the visible and near infrared regions were reported by Gatterer and Krishnamurthy [4] and Vittalachar and Krishnamurthy [5]. In a latter study Gatterer et al. [6] published the spectra of WO in an atlas which also included the spectra of many other transition metal oxides. Some WO bands were also observed in a shock tube [7] but the spectra remained largely unclassified. Weltner and McLeod [8] observed the electronic spectra of WO in Ne and Ar matrices while Green and Ervin [9] measured the ground state vibrational frequency of WO in the Ar and Kr. The visible and near infrared bands observed by Weltner and McLeod [8] have been classified into several transitions which were labeled using letters ranging from A to G. The absorption spectra of WO have also been investigated by Samoilova et al. [10] who maintained the letter notation proposed by Weltner and McLeod [8], and also observed some additional bands. Samoilova et al. [10] obtained a rotational analysis of a number of bands in the visible and provided the first rotational constants for WO. The ground state vibrational constants obtained in this work were consistent with those obtained by Green and Ervin [9] in the matrix isolation spectra. Kuzyakov et al. [11,12] carried out an intracavity electronic absorption study of WO and obtained a rotational analysis of some additional bands and proposed new vibrational assignments in the A–X transition based on isotope shifts. More recently Lorenz et al. [13,14] obtained laser-induced fluorescence measurements of WO in solid neon and extended emission observations into the near infrared. In a recent paper Kraus et al. [15] observed the spectrum of the 0-0 band of the F–X transition by cavity ringdown laser absorption spectroscopy.

* Corresponding author.
E-mail address: rram@u.arizona.edu (R.S. Ram).

0022-2852/$ - see front matter © 2009 Elsevier Inc. All rights reserved.
doi:10.1016/j.jms.2009.04.010

From the observation of the well-resolved tungsten isotopic structure they concluded that the anomalous isotopic splitting was the result of strong interstate interactions. In spite of so many studies, the nature of the ground state of WO had still been in question. Weltner and McLeod [8] suggested a $^3\Sigma^-$ ground state while Nelin and Bauschlicher [16] predicted a $^5\Pi$ ground state from SCF and CASSCF calculations. In our recent study of WO we reported the rotational analysis of a number of transitions and classified the bands into two main groups having $\Omega'' = 0^+$ and $\Omega'' = 1$ lower states with $\Omega'' = 0^+$ state being the lowest [17]. We labeled the two states as $X0^+$ and X1, which are the spin components of the $X^3\Sigma^-$ ground state of WO [17]. In this study our assignment was supported by our own *ab initio* calculations [17]. Very recently Cooke et al. [18] studied WO by microwave spectroscopy and their observations were consistent with $X0^+$ being the lowest state (ground state) of WO.

In the present work we have obtained the analysis of many more emission bands of WO in the 9000–25 000 cm^{-1} interval and report the observation of additional states belonging to the two groups of bands reported earlier [17]. In addition, we also report the rotational analysis of several new bands involving some low-lying states. Some of these states may be components of a low-lying $^5\Pi$ state predicted by our *ab initio* calculations. These observations will be discussed in the light of our most recent *ab initio* calculations.

Table 1
Observed bands involving the low-lying electronic states of WO. The $X0^+$ and X1 states have been assigned the spin components of the $X^3\Sigma^-$ ground state, with $X0^+$ being the lowest.

Transitions	Branches	ν_{00} (cm^{-1})	Observed bands
Group 1, bands involving X0⁺ lower state			
$[7.5]0^+$–$X0^+$	1R, 1P	7538	0-0, 1-1, 1-0
$[11.0]0^+$–$X0^+$	1R, 1P	10 965	0-0, 1-1
A1–$X0^+$	1R, 1P, 1Q	17 165	0-1, 0-0, 1-0, 2-0, 3-1
B1–$X0^+$	1R, 1P, 1Q	17 242	0-1, 0-0, 1-0, 2-1
C1–$X0^+$	1R, 1P, 1Q	19 182	0-2, 1-3, 2-4, 0-1, 1-2, 2-3, 0-0
D1–$X0^+$	1R, 1P, 1Q	20 794	0-1, 1-2, 0-0, 1-1, 1-0, 2-1, 2-0, 3-1
$E0^+$–$X0^+$	1R, 1P	22 418	0-0
$F0^+$–$X0^+$	1R, 1P	23 401	0-1, 0-0, 1-0
$F0^+$–$[4.9]0^+$	1R, 1P	18 494	0-0
Group 2, bands involving X1 lower state			
A′2–X1	2R, 2P, 2Q	15 494	0-0, 1-0
$B'0^+$–X1	1R, 1P, 1Q	19 440	0-2, 0-1, 0-0, 1-0
C′2–X1	2R, 2P, 2Q	19 783	0-1, 0-0
D′1–X1	2R, 2P	21 222	0-1, 0-0
$E'0^-$–X1	1R, 1P, 1Q	20 272	0-0
Group 3, bands involving other low-lying states			
$[a+15.3]0^+$–$[a+5.1]0^+$	1R, 1P	10 236	0-0
$[a+15.3]0^+$–[a+5.6]1	1R, 1P, 1Q	9705	0-0
$[a+15.3]0^+$–[a+5.9]1	1R, 1P, 1Q	9395	0-0
A′2–[a+5.6]1	2R, 2P, 2Q	9877	0-0
[a+19.4]1–$[a+5.1]0^+$	1R, 1P, 1Q	14 336	0-0
[a+19.4]1–$[a+5.4]0^-$	1R, 1P, 1Q	13 988	0-0
[a+20.4]2–[a+5.9]1	2R, 2P, 2Q	14 488	0-0

Note: "a" marks the undetermined separation between $X0^+$ and X1 components of the $X^3\Sigma^-$ ground state.

2. Experimental

The emission bands of WO were produced during a search for WCl bands in an electrodeless microwave discharge through a flowing mixture of WCl_6 vapour and He. Although the WCl bands were not observed, we observed WO bands instead, without adding any O_2 to the mixture presumably as the result of reactions with impurities. The discharge tube was made of quartz and had an outside diameter of 12 mm. The emission from the lamp was sent directly into the entrance aperture of the 1-m Fourier transform spectrometer associated with the McMath-Pierce Telescope of the National Solar Observatory. The spectra were recorded in three parts, 4000–10 000 cm^{-1}, 9000–19 000 cm^{-1} and 17 000–35 000 cm^{-1}. For the 4000–10 000 cm^{-1} region, the spectrometer was equipped with a UV beamsplitter, silicon and green glass filters and liquid nitrogen cooled InSb detectors. The spectra were recorded by coadding 104 scans in about 10 h of integration at 0.025 cm^{-1} resolution. For the other two parts, the spectrometer

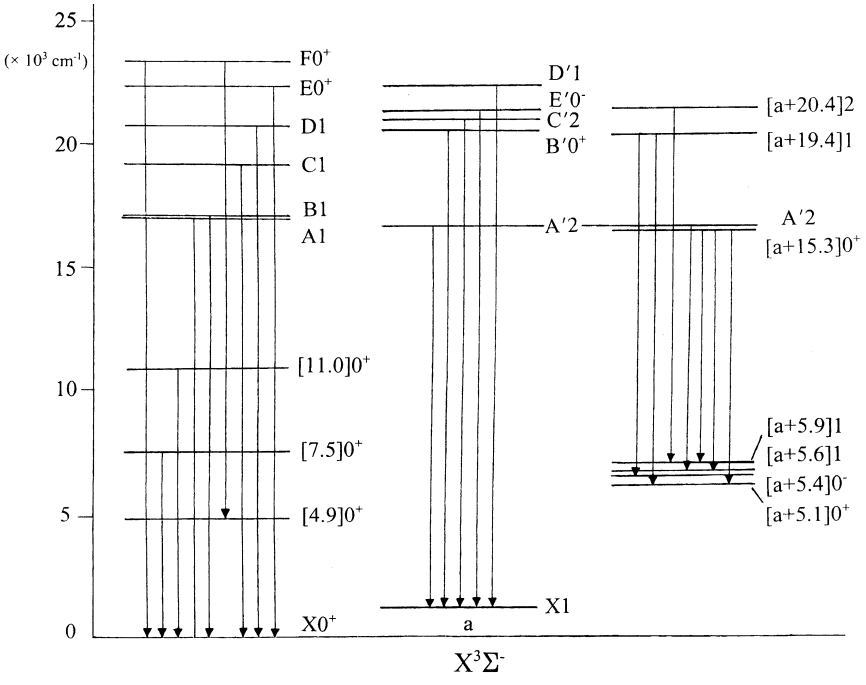

Fig. 1. Schematic energy level diagram of the observed transitions of WO. The $X0^+$ and X1 lower states have been assigned as the spin components of the $X^3\Sigma^-$ ground state of WO.

was also equipped with a UV beamsplitter and silicon photodiode detectors. For the 9000–19 000 cm^{-1} region OG530 red pass filters were used and the spectra were recorded at 0.02 cm^{-1} resolution by coadding 6 scans in 1 h of integration while the 17 000–35 000 cm^{-1} region was recorded using a $CuSO_4$ filter and coadding 6 scans at 0.03 cm^{-1} resolution. The WO bands were also recorded using the Bruker IFS 120 HR Fourier transform spectrometer at Waterloo, but the present analysis was made using the Kitt Peak data. The line positions were extracted from the observed spectra using a data reduction program called PC-DECOMP developed by Brault. The peak positions were determined by fitting a Voigt line shape function to each spectral feature. The WO spectra were calibrated by transferring the calibration from WN lines [19], which were calibrated by using the Ne line measurements of Palmer and Engleman [20]. The WO lines in the stronger bands appear with a maximum signal-to-noise ratio of about thirty and have a typical line width of ~0.05 cm^{-1}. The precision of measurements of strong and unblended WO lines is expected to be better than ±0.003 cm^{-1}. The structure of some WO bands is complex because of resolved (or partly resolved) structure from the four isotopologues, ^{182}WO, ^{183}WO, ^{184}WO and ^{186}WO. The uncertainty of measurements is expected to vary from ±0.002 to ±0.005 cm^{-1} depending upon the signal-to-noise ratio, extent of blending and line broadening.

3. Observation and analysis

Most of the bands observed by Samoilova et al. [10] in the 16 000–25 000 cm^{-1} interval are present in our spectra, but the higher wavenumber bands (>25 000 cm^{-1}) were not observed. The rotational analysis of most of the strong bands has been completed although a few weaker bands still remain to be analyzed. The present observations have been summarized in a schematic energy level diagram provided in Fig. 1, while a list of observed bands belonging to different transitions is provided in Table 1. Our analysis shows that most of the strong bands can be classified into two groups having different lower states. The lower state constants of the two groups are very similar and have been assigned as $\Omega = 0^+$ and $\Omega = 1$ spin components of the $X^3\Sigma^-$ ground state. Sev-

Table 2
Spectroscopic constants (in cm^{-1}) for states in group 1.

State	v	T_v	B_v	$D_v \times 10^6$	$H_v \times 10^{10}$	$L_v \times 10^{13}$	$q_v \times 10^3$	$q_{Dv} \times 10^6$	$q_{Hv} \times 10^9$	$q_{Lv} \times 10^{13}$
	1	24318.5243(17)	0.3811162(62)	0.2855(19)	–	–	–	–	–	–
$F0^+$	0	23401.0801(28)	0.383930(12)	0.467(11)	0.551(33)	–	–	–	–	–
$E0^+$	0	22412.194(11)	0.385625(26)	0.166(13)	–	–	–	–	–	–
	3	23699.8391(14)	0.3831108(55)	0.3004(15)	–	–	−0.5615(22)	−0.03425(83)	–	–
	2	22741.5033(12)	0.3852613(59)	0.3003(19)	–	–	−0.6125(49)	0.0654(23)	–	–
	1	21772.9832(15)	0.3870643(58)	0.2611(18)	–	–	−0.2808(28)	−0.0087(14)	–	
D1	0	20793.8569(11)	0.3889130(59)	0.2436(20)	−0.0115(21)	–	−0.2469(27)	−0.0199(19)	0.00257(32)	–
	2	21031.6341(31)	0.3879669(90)	0.6373(70)	0.775(28)	−0.0750(39)	−2.4792(62)	0.7815(96)	−0.1707(46)	0.1639(69)
	1	20109.7092(22)	0.388227(12)	0.802(22)	−3.75(18)	1.278(46)	1.461(13)	1.126(37)	0.729(33)	−2.533(90)
C1	0	19182.4617(15)	0.3914117(71)	0.2498(53)	-0.046(19)	−0.0477(24)	−0.0190(29)	0.1568(25)	0.06745(50)	–
	2	19211.7718(19)	0.386997(14)	−2.162(32)	−9.32(21)		14.162(21)	−4.273(61)	1.80(42)	–
	1	18227.8756(22)	0.3897094(99)	−0.7249(76)	−0.856(18)		−5.2*			
B1	0	17242.0010(14)	0.3923935(84)	−1.6677(88)	−1.593(34)	–	4.1865(81)	−1.334(14)	0.1521(62)	–
	3	19856.4924(16)	0.3790911(64)	0.3848(27)	–	–	4.7344(49)	−0.0717(43)	–	–
	2	18969.8725(19)	0.3816100(76)	0.5054(37)	–	–	4.7594(58)	0.1220(55)	−0.0433(12)	–
	1	18074.2157(16)	0.3847932(81)	0.8175(58)	0.358(14)	–	4.6229(78)	0.361(11)	−0.0709(50)	0.0547(79)
A1	0	17164.9641(14)	0.3913397(73)	2.1370(60)	1.881(24)	-0.0660(32)	3.4260(57)	1.1384(85)	−0.1876(39)	0.0960(55)
	1	11989.1481(26)	0.411745(20)	0.308(37)	−1.49(19)	–	–	–	–	–
$[11.0]0^+$	0	10965.4450(19)	0.4151496(68)	0.2726(22)		–	–	–	–	–
$[7.5]0^+$	1	8492.1470(48)	0.389984(10)	0.2625(35)	–	–	–	–	–	–
	0	7537.8417(18)	0.3919096(79)	0.2434(56)	−0.027(17)	0.0024(18)	–	–	–	–
$[4.9]0^+$	0	4910.6260(49)	0.403506(18)	0.466(16)	0.409(45)	–	–	–	–	–
	4	4181.9326(31)	0.4074382(72)	0.2636(22)	–	–	–	–	–	–
	3	3148.5456(24)	0.4094774(65)	0.2639(20)	–	–	–	–	–	–
	2	2107.0887(15)	0.4114968(56)	0.2589(16)	–	–	–	–	–	–
	1	1057.56542(86)	0.4135229(53)	0.2570(14)	–	–	–	–	–	–
$X0^+$	0	0.0	0.4155370(54)	0.2554(15)	–	–	–	–	–	–

Note: An asterisk marks a fixed value.

Table 3
Spectroscopic constants (in cm^{-1}) for states in group 2.

State	v	T_v	B_v	$D_v \times 10^7$	$H_v \times 10^{11}$	$q_v \times 10^3$	$q_{Dv} \times 10^8$
D′1	0	a+21222.3006(14)	0.3849270(88)	2.866(24)	–	−1.1572(27)	−2.05(14)
$E'0^-$	0	a+20272.2141(32)	0.384305(18)	3.43(21)	−9.09(75)	–	–
	1	a+20722.2089(20)	0.386097(10)	2.759(32)	–	–	–
C′2	0	a+19782.7931(10)	0.3879773(89)	2.703(24)	–	–	–
	1	a+20386.3362(21)	0.3835848(99)	2.624(29)	–	–	–
$B'0^+$	0	a+19439.6245(11)	0.3854840(89)	2.657(24)	–	–	–
	1	a+16405.5224(13)	0.384924(10)	2.831(58)	−1.12(13)	–	−2.538(69)
A′2	0	a+15493.9585(44)	0.386440(30)	2.42(33)	–	–	–
	2	a+2111.7994(30)	0.412195(10)	2.487(31)	–	0.162*	–
	1	a+1059.9311(10)	0.4142196(90)	2.484(25)	–	0.16228(36)	–
X1	0	a	0.4162385(89)	2.480(24)	–	0.16254(56)	

Note: "a" marks the undetermined separation between $X0^+$ and X1 components of the $X^3\Sigma^-$ ground state, while an asterisk marks a fixed value (see text for details).

Table 4
Spectroscopic constants (in cm^{-1}) for states belonging to group 3.

State	v	T_v	B_v	$D_v \times 10^7$	$H_v \times 10^{11}$	$q_v \times 10^3$	$q_{Dv} \times 10^8$
[a+20.4]2	0	a+20411.3844(22)	0.377243(56)	1.550(38)	–	–	–
[a+19.4]1	0	a+19422.1680(25)	0.3750801(73)	1.459(45)	–	−0.1670(30)	−0.45(16)
A′2	0	a+15493.9585*	0.386440*	2.42*	–	–	–
[a+15.3]0^+	0	a+15321.6912(17)	0.3911750(57)	4.939(44)	1.179(33)	–	–
[a+5.9]1	0	a+5926.7980(21)	0.3948424(65)	1.998(52)	−0.114(75)	−2.5222(22)	1.29(12)
[a+5.6]1	0	a+5617.2745(11)	0.3946026(46)	1.996(38)	–	1.2810(35)	−0.97(27)
[a+5.4]0^-	0	a+5434.7160(29)	0.3917813(84)	1.541(51)	–	–	–
[a+5.1]0^+	0	a+5086.0463(22)	0.3926388(73)	1.645(48)	–	–	–

Note: "a" marks the undetermined separation between $X0^+$ and X1 components of the $X^3\Sigma^-$ ground state, while an asterisk marks a fixed value.

eral other bands involving low-lying states have also been observed in the 9000–15 000 cm^{-1} region.

A majority of WO bands show a W isotopic splitting; the W atom has four main isotopes, ^{182}W (26.3%), ^{183}W (14.3%), ^{184}W (30.7%) and ^{186}W (28.6%). In the present work we have obtained a rotational analysis for the most abundant ^{184}WO isotopologue. The branches in different WO bands were sorted out using a color Loomis–Wood program, which is very helpful in identifying the rotational lines in the weaker and overlapped bands. The rotational assignment in these bands was obtained by comparing the combination differences for the common vibrational levels. While determining the spectroscopic constants, the overlapped or blended lines were given reduced weights. Rotational lines affected by perturbations were given reduced weights or were deweighted completely. The rotational constants were determined by fitting simultaneously the lines to the customary energy level expression:(for $\Omega = 0^+$ states)

$$F_v(J) = T_v + B_v J(J+1) - D_v[J(J+1)]^2 + H_v[J(J+1)]^3 + L_v[J(J+1)]^4 \quad (1)$$

(for $\Omega = 1$ states)

$$F_v(J) = T_v + B_v J(J+1) - D_v[J(J+1)]^2 + H_v[J(J+1)]^3 + L_v[J(J+1)]^4 \pm 1/2\{qJ(J+1) + q_D[J(J+1)]^2 + q_H[J(J+1)]^3 + q_L[J(J+1)]^4\}. \quad (2)$$

The constants obtained for the electronic states belonging to groups 1, 2 and 3 are provided in Tables 2–4, respectively. The description of observed WO bands will be provided in the following sections.

3.1. Group I, bands with an $X0^+$ lower state

The first group consists of nine transitions out of which eight have a common $\Omega = 0^+$ lower state. We have labeled this state as $X0^+$. The transitions with the $X0^+$ common lower state have their band origins near 7538 cm^{-1} ([7.5]0^+–$X0^+$), 10 965 cm^{-1} ([11.0]0^+–$X0^+$), 17 165 cm^{-1} (A1–$X0^+$), 17 241 cm^{-1} (B1–$X0^+$), 19 182 cm^{-1} (C1–$X0^+$), 20 793 cm^{-1} (D1–$X0^+$), 22 418 cm^{-1} ($E0^+$–$X0^+$) and 23 401 cm^{-1} ($F0^+$–$X0^+$). Most of these transitions were also observed by the relaxed laser-induced fluorescence measurements of Lorenz et al. [12,13] and the matrix isolation absorption experiment of Weltner and McLeod [8]. This suggests that the common lower state of these transitions is certainly the ground state of WO. This assignment was also confirmed by the microwave experiments of Cooke et al. [18].

3.1.1. The [7.5]0^+–$X0^+$ transition

Two bands observed with origins near 7400, 7538 and 8385 cm^{-1} have been assigned as the 1-1, 0-0 and 1-0 band of a $\Delta\Omega = 0$ transition with $X0^+$ state as its lower state. The 0-0 band is much stronger than the 1-1 and 1-0 bands. The bands belonging to this transition consist of single R and P branches, typical for a $\Delta\Omega = 0$ transition. The lower state combination differences from these bands match very well with those of the $v = 0$ and 1 vibrational levels of the common $X0^+$ state. This assignment places the 0-1 and 1-0 bands of this transition at 6480 and 8492 cm^{-1}. Very weak bands with R heads at 6488 and 8499 cm^{-1} have, therefore, been assigned as the 0-1 and 1-0 band of this transition. The 0-1 band is too weak in intensity to be analyzed rotationally. However, the rotational lines of the 1-0 band were easily picked out in the spectrum using the predictions based on the constants obtained

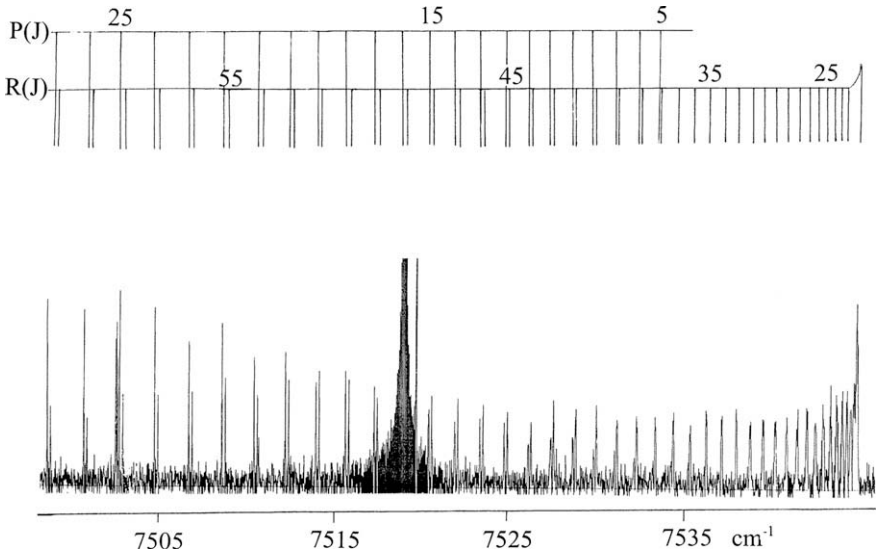

Fig. 2. A portion of the spectrum of the [7.5]0^+–$X0^+$, 0-0 band of WO marking some low J lines of the R and P branches. The strong feature at the center is a He line.

from the analysis of the 0-0 and 1-1 bands. A part of the spectrum of the 0-0 band near the R head has been provided in Fig. 2, in which some R and P lines have been marked. The apparent broadening in the lower-J lines of this band arises from partially resolved isotope splitting. ^{182}W–^{184}W and ^{184}W–^{186}W isotope shifts of ~0.46 cm^{-1} have been observed in the 1-0 band consistent with its assignment. Rotational lines up to R(70) and P(56) have been assigned in the 0-0 band.

3.1.2. The [11.0]0$^+$–X0$^+$ transition

To higher wavenumbers, another $\Delta\Omega = 0$ transition has been identified with the 0-0 band near 10 965 cm^{-1}. The rotational structure of this band has an open structure with the R and P branches moving in opposite directions with increasing J quantum numbers. This suggests that the rotational constants for the upper and lower states are similar. The 1-1 band with an origin near 10 931 cm^{-1} was also rotationally analyzed. No isotope shift has been observed in these bands although some broadening, most probably due to partial isotope splitting, has been observed for higher J rotational lines. The analysis of the 0-0 and 1-1 bands of this transition provides $\Delta G_{1/2} = 1024$ cm^{-1} for the [11.0]0$^+$ state, although the 0-1 or 1-0 bands were not observed in our spectra.

3.1.3. The A1–X0$^+$ transition

Five bands with origins near 16 107, 17 165, 18 074, 18 798 and 18 970 cm^{-1}, have been assigned as the 0-1, 0-0, 1-0, 3-1 and 2-0 bands, respectively, of a transition which has been labeled as A1–X0$^+$. All of these bands have been rotationally analyzed. These bands were also observed by Weltner and McLeod [8] and Samoilova et al. [10] but their vibrational assignment differs from ours. Samoilova et al. [10] assigned the current 0-1, 0-0, 1-0 and 2-0 bands as 3-0, 3-1, 4-0 and 5-0 bands. A search for other vibrational bands based on their assignment was unsuccessful and the bands were not present at the predicted positions. The assignments of Weltner and McLeod [8] were also found to be incorrect. The discrepancy in the vibrational assignments is due to peculiar isotope effects. ^{186}W–^{184}W–^{182}W isotope shifts of −0.24, −0.69 and −0.85 cm^{-1} have, respectively, been measured for the 0-1, 0-0 and 1-0 bands. The observation of such a large isotope shift for a 0-0 band is highly unusual. This anomalous isotope effect is the result of strong interactions in the excited state, which shifts the different isotopologues by different amounts. In fact, based on abnormal isotope effects, Kuzykov et al. [11,12] wrongly reassigned the 3-1 (current 0-1) and 3-0 (current 0-0) bands of the A1–X0$^+$ system as 0-0 and 1-0 bands. Their revised assignment leads to an excited state vibrational interval $\Delta G'_{1/2}$ of 1057.41 cm^{-1}, which is actually the vibrational interval in the X0$^+$ ground state. Their rotational analysis of the 16 107 and 17 165 bands is also incorrect. The spectrum of each band belonging to this transition consists of R, P and Q branches as expected for a $\Delta\Omega = 1$ transition. An expanded portion of the spectrum of the 0-0 band is provided in Fig. 3, where some rotational lines belonging to the Q branches of the isotopologues ^{186}WO, ^{184}WO and ^{182}WO have been marked.

3.1.4. The B1–X0$^+$ transition

Another group of four bands with origins near 16 184, 17 242, 18 154 and 18 228 cm^{-1} have been assigned as the 0-1, 0-0, 2-1 and 1-0 bands of a different transition. This transition has been labeled as the B1–X0$^+$ following the notation used by Samoilova et al. [10] and Weltner and McLeod [8]. The present vibrational assignment also agrees with the assignments of Samoilova et al. [10] and Weltner and McLeod [8]. All of the bands mentioned above, have been rotationally analyzed. The rotational structure of bands belonging to this transition consists of a single R, a single P and a single Q branch. As found for the A1–X0$^+$ transition, the B1–X0$^+$ bands also exhibit abnormal isotope effects. For example the ^{186}WO–^{184}WO isotope shifts of −0.19, −0.67 and −1.34 cm^{-1} were observed, respectively, for the 0-1, 0-0 and 1-0 bands. The abnormal isotope splitting in these bands is again attributed to interactions in the excited state.

3.1.5. The C1–X0$^+$ transition

To higher wavenumbers, a group of seven bands has been identified as belonging to a different electronic transition labeled as C1–X0$^+$. This transition has the most extensive vibrational structure of all the transitions of WO with bands up to $v'' = 4$ of the ground state. The bands with origins near 16 850, 16 961, 17 075, 17 883, 18 003, 18 124 and 19 182 cm^{-1} have been assigned as the 2-4, 1-3, 0-2, 2-3, 1-2, 0-1 and 0-0, respectively, all of which have been rotationally analyzed. The bands of this transition also show unusual isotope effects like the A1–X0$^+$ and B1–X0$^+$ bands.

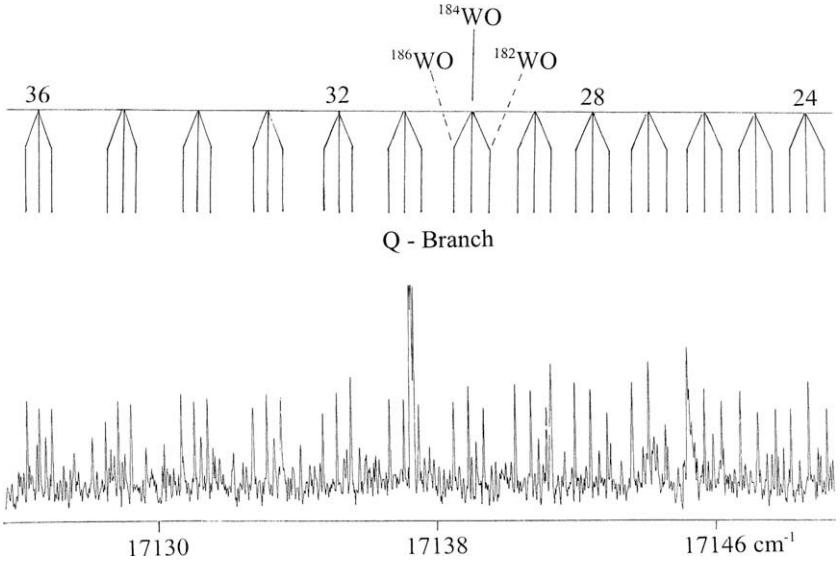

Fig. 3. A portion of the spectrum of the 0-0 band of the A1–X0$^+$ transition, marking some lines in the Q branch. The isotopic lines of the most abundant isotopomers, ^{186}WO, ^{184}WO, and ^{182}WO, have been marked. The lines belonging to the weaker isotopomer ^{183}WO, are present in between ^{184}WO and ^{182}WO, but have not been marked.

For example an ^{186}WO–^{184}WO isotope shift of -0.26 cm^{-1} has been observed near the band origin of the 0-0 band. It has been noted that the ^{186}WO–^{184}WO–^{182}WO isotope splitting decreases with increasing J values and lines of the three main isotopologues eventually merge near $J = \sim 50$. A compressed portion of the spectrum of the 0-0 band is presented in Fig. 4. Although individual rotational lines have not been marked, isotopic structure is clearly resolved even in the 0-0 band.

3.1.6. The D1–X0$^+$ transition

Another transition with a 0-0 band origin near 20 794 cm^{-1} has been identified. The 0-0 band of this transition is strongest of the observed WO bands. A small ^{186}WO–^{184}WO isotope shift of about -0.07 cm^{-1} has been observed even in the 0-0 band. In total, eight bands involving vibrational levels $v' = 0$-3 and $v'' = 0$-2 have been identified and rotationally analyzed. A portion of the 0-0 band of the D1–X0$^+$ transition is presented in Fig. 5, where the much weaker R head of the 1-1 band has also been marked. The 1-1 band is partly overlapped by the 0-1 band of the C′2–X1system as shown in the Figure.

Bands belonging to this transition consist of a single R, a single P and a single Q branch, with the Q branch being the most intense. As mentioned by Samoilova et al. [10], a perturbation in the $v' = 2$ vibrational level of the D1 state has been found in the analysis of the 2-0 and 2-1 bands. The f-parity levels of the $v' = 2$ vibrational level are perturbed near $J = 25$ and a number of rotational lines in the vicinity of perturbation were deweighted in the final fit.

3.1.7. The E0$^+$–X0$^+$ transition

A weak $\Delta\Omega = 0$ band with an origin near 22 412 cm^{-1} has been assigned as the 0-0 band of the E0$^+$–X0$^+$ transition. This band has a small isotope shift which is only partly resolved in our spectra. This band was assigned as 1-0 by Samoilova et al. [10] based on their lower resolution spectra and other bands with R heads near 23 430.2, 24 356.9 and 25 222.5 cm^{-1} were assigned by them as 2-0, 3-0 and 4-0. The assignment of Samoilova et al. [10] provides $\Delta G_{3/2}$, $\Delta G_{5/2}$ and $\Delta G_{7/2}$ values of 1012, 927 and 1166 cm^{-1}, which is possible only if the excited state is strongly perturbed (or the bands were miss-assigned). The 0-0 and other vibrational bands predicted based on this assignment of Samoilova et al. [10] were

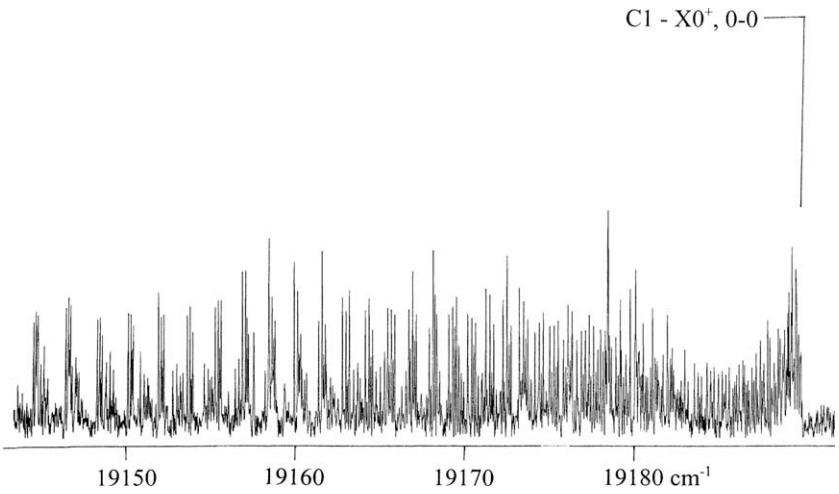

Fig. 4. A compressed portion of the 0-0 band of the C1–X0$^+$ transition providing an overall view of this band. The isotope splitting due to the most abundant isotopomers can clearly be seen in the spectrum, although the individual lines have not been marked.

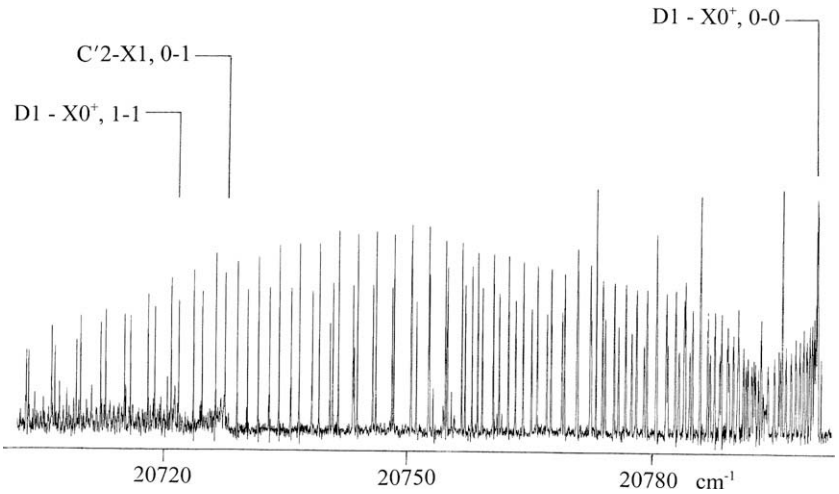

Fig. 5. A portion of the 0-0 band of the D1–X0$^+$ transition of WO near the band head. Very weak R heads of the 1-1 band of the D1–X0$^+$ system as well as the 0-1 band of the C′2-X1 system have also been marked.

not observed by us. The only observed band at 22 412 cm^{-1} has, therefore, been assigned as the 0-0 band of the $E0^+$–$X0^+$ transition.

3.1.8. The $F0^+$–$X0^+$ and $F0^+$–[4.9]0^+ transitions

Two 0-0 bands having a common upper state have been observed at 23 401 and 18 490 cm^{-1}. The lower state of the 23 401 cm^{-1} band is the $X0^+$ ground state of WO and the 0-1 and 1-0 bands have also been measured and rotationally analyzed. However, the lower state of the 18 490 cm^{-1} band is not common to any other known state and involves a new $\Omega = 0^+$ state. Our rotational analysis places this new state at 4910.6 cm^{-1} above the ground $X0^+$ state. No other vibrational levels associated with this transition could be identified in our spectra, and it is possible that the upper state is in fact not the $F0^+$ state.

3.2. Group II, bands with an X1 lower state

The second group of bands consists of several transitions which have an $\Omega'' = 1$ state as the lower state (see Fig. 1). This lower state has been labeled as X1. Five transitions, labeled as A′2–X1, B′0^+–X1, C′2–X1, D′1–X1 and E′0^+–X1 have been identified as belonging to this group. The fact that none of the bands in the second group were observed in a matrix absorption experiment [8] suggests that the lower state of group 2 is well above the $X0^+$ ground state. Supported by our *ab initio* calculations, we have assigned the $X0^+$ and X1 states as the spin components of the $X^3\Sigma^-$ ground state of WO. We have not been able to determine the separation between the $X0^+$ and X1 states.

3.2.1. The A′2–X1 transition

Two bands located near 15 494 and 16 406 cm^{-1} have been assigned as 0-0 and 1-0 bands of the A′2–X1 transition. None of these bands were observed in the matrix isolation spectra of Weltner and McLeod [8] as well as previous low resolution studies by Gatterer et al. [4,6] and Vittalachar and Krishnamirthy [5]. Samoilova et al. [10] observed a band with an R head near 16 410.1 cm^{-1} (the current 1-0 band) but left it unassigned. The bands belonging to this transition consist of two R, two P and two Q branches. Rotational analysis of these bands was obtained by comparing the lower state combination differences with the corresponding values from other transitions of this group. A local perturbation was identified in the $v' = 0$ vibrational level of the excited state near $J = 30$ which affects both parity components. Several rotational lines in the perturbation region were deweighted in our fits. The 1-0 band is free from perturbation and rotational lines up to R(41), P(50) and Q(56) were observed in this band.

3.2.2. The B′0^+–X1 transition

On the higher wavenumber side, four bands with origins near 17 328, 18 381, 19 440 and 20 386 cm^{-1} have been assigned as the 0-2, 0-1, 0-0 and 1-0 bands of the B′0^+–X1 transition. None of these bands were observed in previous studies of WO except the 0-1 band, which was listed by Samoilova et al. [10] but was left unassigned. Bands belonging to this transition consist of a single R, a single P and a single Q branch. All of these bands have been rotationally analyzed and were found to be free from local perturbations. In the 0-2 band we were able to identify only the lines in the Q branch and therefore, the Ω-doubling constant was held fixed at the value for $v = 1$ of the ground state.

3.2.3. The C′2–X1 transition

Three bands located near 18 724, 19 783 and 20 722 cm^{-1} have been assigned as the 0-1, 0-0 and 1-0 bands of the C′2–X1 transition. The 0-1 and 0-0 bands were previously observed by Samoilova et al. [10], but no rotational analysis was carried out. The rotational structure of the bands consists of two R, two P and two Q branches. The 1-0 band is much weaker and the lines only in the Q branch were measured with certainty and included in the determination of the spectroscopic constants. These bands are free from local perturbations.

3.2.4. The D′1–X1 transition

Three bands located near 20 163, 21 222 and 22 102 cm^{-1} have been assigned as the 0-1, 0-0 and 1-0 bands of the D′1–X1 transition. These bands were also observed in the absorption spectrum of Samoilova et al. [10]. The spectrum of these bands consists of two R and two P branches which were easily assigned. Unlike most of the WO bands belonging to group 1, no isotope splitting has been observed in the 0-0 band. An expanded portion of the spectrum of the 0-0 band marking some R and P branches is presented in Fig. 6. No rotational perturbation has been observed in the bands belonging to this transition.

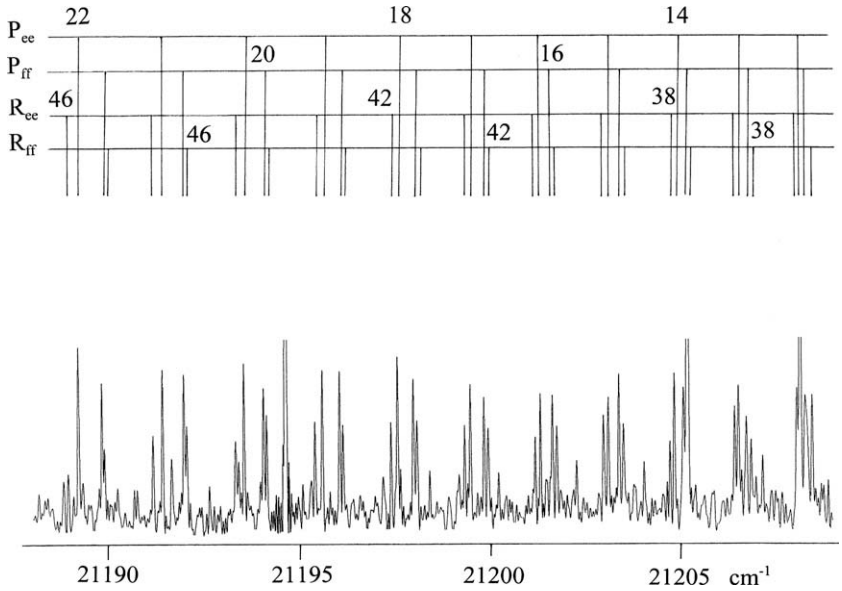

Fig. 6. An expanded portion of the D′1–X1, 0-0 band marking some lines in the R and P branches. The lines are split into two components due to presence of Ω-doubling in both states.

3.2.5. The E′0⁺–X1 transition

A 0-0 band appearing with weak intensity has been observed in our spectrum near 20 272 cm^{-1}. This band was not observed either by Weltner and McLeod [8] or by Samoilova et al. [10]. The spectrum of this band consists of a single R, a single P and a single Q branch. Rotational analysis of this band results in a $\Omega'' = 0^-$ assignment for the upper state. No other vibrational bands were observed associated with this transition.

3.3. Group III, bands involving other low-lying states

Several additional WO bands have been observed in the lower wavenumber region extending into the near infrared. These bands are interconnected by common vibrational levels. The most prominent bands of this group are located near 9395, 9705, 9877, 10 236, 13 988, 14 336 and 14 488 cm^{-1}. Most of these bands are the 0-0 bands of different transitions. Bands located in the 9000–10 000 cm^{-1} interval have been observed for the first time. Rotational analysis of most of the stronger bands has been obtained but some weaker bands remain still unassigned. After comparing the rotational constants we have concluded that the 10 408 and 15 494 cm^{-1} bands have their upper states in common. The common upper state has been identified as the A′2 state (Table 3). This observation provides the location of other low-lying states, [a+5.1]0^+, [a+5.4]0^-, [a+5.6]1, [a+5.9]1, [a+15.3]0^+, [a+19.4]1 and [a+20.4]2, relative to the X1 state (Fig. 1).

Among the group 3 bands, the 0-0 band at 10 236 cm^{-1} appears interesting because of its open rotational structure. This band consists of a single R and a single P branch which move in the opposite direction with increasing J because of the near equality of rotational constants in the upper and lower states. The 1-1 band associated with this transition is also present weakly but was not assigned due to lack of sufficient data. This band has been assigned as a 0^+-0^+ transition with the lower state assigned as the [a+5.1]0^+ state. A part of the 0-0 band is presented in Fig. 7 where a few R and P lines near the band origin have been marked. No isotope shift has been observed in this band, although some broadening was noticed for high J lines probably due to isotopic effects. The upper state of this transition also has transitions to two other low-lying states, [a+5.6]1 and [a+5.9]1. Another near infrared band observed at 9877 cm^{-1} has been assigned as an $\Omega = 2$–$\Omega = 1$ transition with the upper state being the A′2 state. Notice that the absolute parity of the group 3 states has not been determined because the connecting $v = 0$ A′2 state does not have resolved Ω doubling. This means that all of the parities in group 3 can be changed (e–f and f–e) without changing the quality of the fit. This parity inversion changes the sign of all Ω doubling constants and changes 0^+ into 0^- (and 0^- into 0^+).

4. *Ab initio* results and electronic structure of WO

In a previous study of WO we reported the results of our CMRCI *ab initio* calculations aimed at predicting the spectroscopic properties of the low-lying electronic states [17]. The goal of that paper was to assign the $\Omega = 0^+$ and 1 components of the $^3\Sigma^-$ ground state, so we focused our calculations on the very few low-lying electronic states in each spin manifold (the 4 lower triplets and the lowest quintet and septet states). It was presumed that the singlet electronic states lie much higher in energy and they were not included. The observation of some additional transitions of WO in the near infrared led us to believe that a more comprehensive *ab initio* effort was needed, aiming at characterizing all states occurring in the energy window below 25 000 cm^{-1}.

The calculations were carried out in three successive steps as detailed below. In the first step, we completed the calculations of our previous work [17], adopting the same computational scheme. The results provide a first global survey of the (Λ, S) electronic structure of WO within the considered energy range. In a second step, we performed vertical energy calculations at a higher level of theory, in order to improve the accuracy of the predicted energies. Finally, we introduced spin–orbit coupling into the calculation and predicted a relative energy scale of all Ω states below 25 000 cm^{-1}.

All calculations carried out in this work have been performed with the MOLPRO program [21] running on the HP-XC 4000 cluster of the ULB/VUB computing center, using the internally Contracted Multi-Reference Configuration Interaction method (CMRCI) [22,23] with explicit correlation of all valence electrons. The CASSCF active space is defined by the four σ, two π and one δ molecular orbitals correlating to the atomic valence shells. All energies are corrected for unlinked quadruple excitations [24].

In the first set of CMRCI calculations, hereafter referred to as CMRCI (I), we used the standard basis sets and quasi-relativistic small core potentials from the Stuttgard library for both atoms [25,26]. The basis sets are augmented by a single polarization Gaussian on each atom (f and d on W and O, respectively). All possible spatial ($0 \leqslant \Lambda \leqslant 6$) and spin ($0 \leqslant S \leqslant 3$) symmetries were considered in the calculations and all states below 30 000 cm^{-1} should

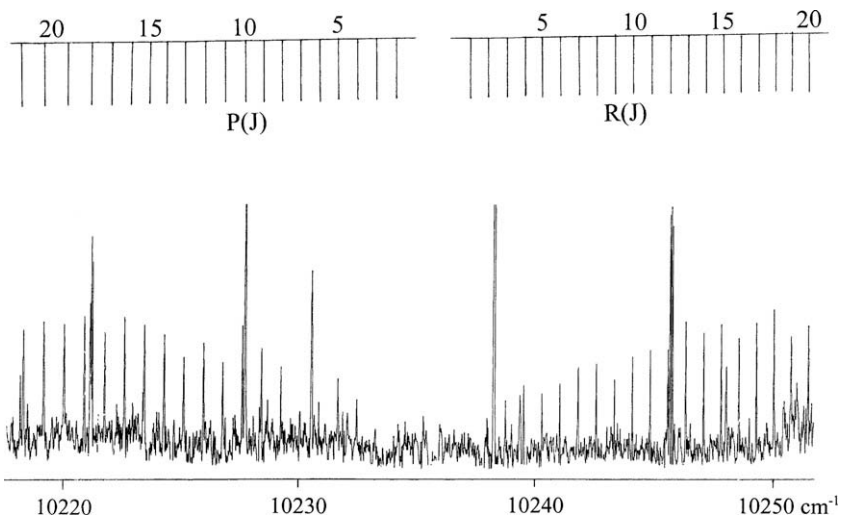

Fig. 7. An expanded portion of the [a+15.3]0^+–[a+5.1]0^+, 0-0 band marking some low J, R and P lines.

be calculated. We systematically checked that the highest calculated state of any symmetry species lies outside of the energy window of interest. The CMRCI (I) results for the 25 lowest (Λ, S) states are reported in Table 5. The equilibrium geometries were determined by gradient optimizations achieved at the CMRCI level of theory, providing the T_e and r_e values listed in the Table. For the sake of completeness we also report two states of high spin ($^7\Delta$ and $^7\Sigma^+$) located outside of the energy window. The main electronic configurations describing the calculated states, obtained from the analysis of the CMRCI wave functions, are reported in Table 6. As can be noted, most of the low-lying electronic states can be described by configurations (A–D). Fig. 8 illustrates the energy spacing of all electronic states arising from these configurations that have been characterized at CMRCI level. The electrostatic splitting of the states arising from configurations (A–D) with respect to their respective barycentric energies are also illustrated in Fig. 8. The configuration energy order can easily be explained by a simple picture in which the four external electrons are distributed in the 3σ, 1δ and 2π molecular orbitals. These orbitals are sufficiently separated in energy to provide the energy pattern observed in Fig. 8: configurations (B–D) are obtained from single electron promotions from the ground configuration (A). We find that the 4σ orbital does not really take part in the low-lying electronic structure of WO, as it does in other transition metal diatomics we studied in the past [27,28]. The reason is the strong antibonding character of this orbital that correlates with the tungsten 6s atomic orbital.

Apart from the numerous singly-excited states already mentioned, our calculations also reveal the existence of few doubly excited states in the considered energy window. The $2\ ^1\Sigma^+$ state is the only state of low spin to be predicted below 35 000 cm^{-1}. This state arises from configuration (J), which is expected to be a low-lying doubly excited configuration, promoting 2 electrons from 3σ to 1δ. All other calculated doubly excited states (configurations (F–I)) are high spin states, quintets or septets, stabilized by the electron unpairing. Another general result provided by the analysis of the CMRCI wave functions is the absence of configuration mixing, which can be explained by the large configuration splitting. One could thus conclude that the electronic structure of WO is quite simple and should be correctly described by our CMRCI calculations. The importance of the basis set, electron correlation and relativistic effects motivated us however to run further calculations at a higher level of theory.

Larger scale CMRCI calculations, to be referred to below as CMRCI (II), were thus performed in a second step. We decided to fix the internuclear distance to a value of 1.69 Å, corresponding

Table 5
Spectroscopic properties of the low-lying electronic states of WO from CMRCI (I) calculations.

State	T_e (cm^{-1})[a]	r_e (Å)	Main configuration weights[b]
X $^3\Sigma^-$	0	1.672	83% (A)
1 $^1\Gamma$	7256	1.666	84% (A) + 3% (B)
1 $^1\Sigma^+$	7982	1.669	79% (A) + 4% (J)
1 $^5\Pi$	9463	1.716	84% (D)
1 $^3\Delta$	11 903	1.682	81% (B) + 4%(E)
1 $^3\Pi$	15 043	1.708	73% (C) + 7% (D) + 3%(K)
1 $^3\Phi$	15 077	1.713	54% (C) + 24%(D) + 4% (K)
1 $^1\Delta$	19 551	1.678	82% (B)
1 $^1\Pi$	20 822	1.710	75%(C) + 6% (D)
1 $^1\Phi$	23 081	1.707	67% (C) + 8% (D)
1 ^{3}H	23 313	1.707	85% (D)
2 $^3\Pi$	23 566	1.735	70% (D) + 14% (C)
1 $^5\Delta$	23 881	1.758	87% (G)
2 $^3\Phi$	25 745	1.715	75% (D) + 5% (C) + 3% (K)
3 $^3\Pi$	25 846	1.714	69% (D) + 8% (C) + 5% (K)
4 $^3\Pi$	26 989	1.712	80% (D)
1 ^{1}H	30 036	1.732	86% (D)
2 $^1\Pi$	30 296	1.731	77% (D) + 5% (J)
2 $^1\Phi$	30 685	1.733	15% (C) + 66% (D)
1 $^5\Sigma^+$	31 427	1.771	86% (H)
1 $^7\Pi$	33 882	2.022	92% (F)
3 $^1\Pi$	35 307	1.709	73% (D) + 6% (C)
2 $^1\Sigma^+$	33 915	1.694	75% (J) + 4% (A)
1 $^7\Delta$	41 964	2.005	49% (I) + 24% (L)
1 $^7\Sigma$	47 483	1.981	95% (I)

[a] Adiabatic term energies calculated from optimized CMRCI geometries.
[b] Weights (in percent) are obtained from the sum of squares of the corresponding configuration interaction coefficients. Configurations having a weight lower than 3 percent are not reported. Configuration labeling is defined in Table 6.

Table 6
Electronic configurations describing the low-lying electronic states of WO (see Table 5).

Label	Configuration[a]	Electron promotion[b]
(A)	$1\sigma^2\ 2\sigma^2\ 1\pi^4\ 3\sigma^2\ 1\delta^2$	
(B)	$1\sigma^2\ 2\sigma^2\ 1\pi^4\ 3\sigma^1\ 1\delta^3$	$3\sigma \rightarrow 1\delta$
(C)	$1\sigma^2\ 2\sigma^2\ 1\pi^4\ 3\sigma^2\ 1\delta^1\ 2\pi^1$	$1\delta \rightarrow 2\pi$
(D)	$1\sigma^2\ 2\sigma^2\ 1\pi^4\ 3\sigma^1\ 1\delta^2\ 2\pi^1$	$3\sigma \rightarrow 2\pi$
(E)	$1\sigma^2\ 2\sigma^2\ 1\pi^4\ 3\sigma^1\ 1\delta^2\ 4\sigma^1$	$3\sigma \rightarrow 4\sigma$
(F)	$1\sigma^2\ 2\sigma^2\ 1\pi^3\ 3\sigma^1\ 1\delta^2\ 2\pi^2$	$1\pi\ 3\sigma \rightarrow 2\pi^2$
(G)	$1\sigma^2\ 2\sigma^2\ 1\pi^4\ 3\sigma^1\ 1\delta^1\ 2\pi^2$	$3\sigma\ 1\delta \rightarrow 2\pi^2$
(H)	$1\sigma^2\ 2\sigma^2\ 1\pi^4\ 1\delta^2\ 2\pi^2$	$3\sigma^2 \rightarrow 2\pi^2$
(I)	$1\sigma^2\ 2\sigma^1\ 1\pi^4\ 3\sigma^1\ 1\delta^2\ 2\pi^2$	$2\sigma\ 3\sigma \rightarrow 2\pi^2$
(J)	$1\sigma^2\ 2\sigma^2\ 1\pi^4\ 1\delta^4$	$3\sigma^2 \rightarrow 1\delta^2$
(K)	$1\sigma^2\ 2\sigma^2\ 1\pi^4\ 1\delta^3\ 2\pi^1$	$3\sigma^2 \rightarrow 1\delta\ 2\pi$
(L)	$1\sigma^1\ 2\sigma^2\ 1\pi^4\ 3\sigma^1\ 1\delta^2\ 2\pi^2$	$1\sigma\ 3\sigma \rightarrow 2\pi^2$

[a] Valence electronic configurations.
[b] Electron promotions are defined with respect to the ground electronic configuration (A).

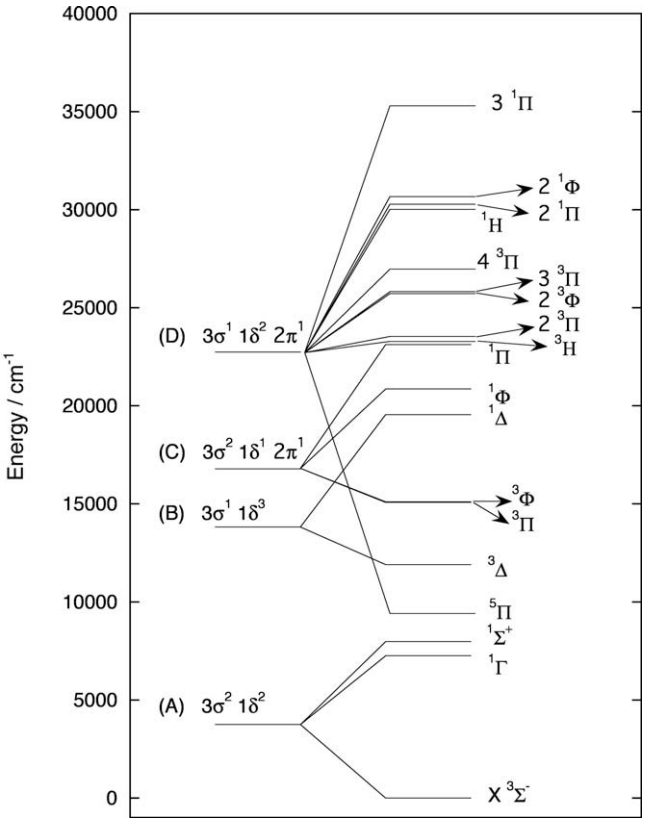

Fig. 8. The low-lying electronic states of WO described by electronic configurations (A–D) [Table 6] from CMRCI calculations.

to the mean equilibrium distance over all states calculated below 20 000 cm^{-1}. The level of calculation has been improved in the following way: (i) the (2*f* 1*g*) polarization set optimized by Martin et al. [29] for tungsten has been used to complete the Stuttgard small core basis set [25]; (ii) the core potential description of oxygen has been replaced by the Dunning *all-electron* cc-pVTZ basis set, recommended in Ref. [29] to be used in combination with the basis set adopted in (i) for W; and (iii) systematic test calculations were performed to define the state average CASSCF orbital optimizations that ensure a balanced description of the different calculated electronic states. These larger scale vertical CMRCI (II) calculations were applied to all states predicted in the first step to lie below 25 000 cm^{-1}. The overall effect of these improvements is a stabilization of the excited states energies, mainly due to an overestimation of the stability of the states arising from the ground configuration. The new vertical energy scale given in Table 7 is thus expected to be more accurate than the one predicted by our first set of calculations. The configuration weights from the analysis of the CMRCI wave functions are not reported because they are found to differ by less than 2% from those given in Table 5.

The final step in our *ab initio* work has been to introduce the spin–orbit (SO) coupling, and to provide a new energy scale taking the spin–orbit splitting into account. The calculations have been carried out at the same internuclear distance of 1.69 Å as before. Let us point out that scalar relativistic effects were already accounted for in all calculations reported above, through the energy-consistent scalar-relativistic pseudopotential that was used for tungsten [25]. This pseudopotential has been supplemented by the corresponding spin–orbit potential [25]. The spin–orbit matrix has been calculated on the basis of the state average CASSCF eigen-functions corresponding to all (Λ, *S*) states encountered within the energy window 0–25 000 cm^{-1}. This matrix has been diagonalized by application of the so-called state interacting method [30], implemented in MOLPRO, and the eigen-solutions corresponding to the resulting Ω states have been analyzed by means of a homemade program. Different authors [31] propose an effective Hamiltonian approach in which the diagonal of the SO matrix is calculated at a higher level of theory than the off-diagonal elements, in order benefit from the better known energy positions of the interacting zeroth order states. This is what we did by replacing the diagonal elements of the spin-orbit matrix of the zeroth-order CASSCF energies by the corresponding CMRCI energies, calculated in the second step. The effects of dynamic correlation are thus incorporated in the energy positions of the interacting states. Table 8 reports the calculated SO energies together with the corresponding Ω values and the main (Λ, *S*) components determined from the analysis of the SO eigenvectors. These results are reported in Fig. 9 where the SO splitting can be visualized. Of particular interest is the value of *a*, the separation between $X0^+$ and X1, which is predicted by the *ab initio* calculations to be as large as 1898 cm^{-1}. This value essentially comes from a strong SO interaction between the $\Omega = 0^+$ components of the $X\ ^3\Sigma^-$ and $1\ ^1\Sigma^+$ states. As will be seen in the discussion, a smaller value ($a = 414\ cm^{-1}$) has been estimated from the observed Ω-doubling in the X1 state. This indirect estimate makes the rather dubious approximation of an isolated $X\ ^3\Sigma^-$ state with interacting $X0^+$ and X1 spin components. However, SO calculations on such systems are also challenging, so it has not been possible to determine if the discrepancy between the two values comes mainly from theory or "experiment". For these values of a, two columns are thus provided in Table 8 to compare the calculated term energies with the observed ones.

As concluded in our previous paper on WO [17], the ground state has been established as a $^3\Sigma^-$ state based on our experimental results supported by the *ab initio* calculations. This is confirmed by the larger scale calculations presented in this work. The first excited state is predicted to be a $^5\Pi$ state, having four close-lying Ω components ($\Omega = 0^-, 0^+, 1, 1$) that can be assigned to the observed [a+5.4]0^-, [a+5.1]0^+, [a+5.6]1 and [a+5.9]1 states, respectively. Note that the $\Omega = 2$ and 3 components of the $^5\Pi$ state are found to be at higher energies, the latter being mixed with the $^3\Delta$ state.

Table 7
Vertical term energies of the low-lying electronic states of WO from CMRCI (II) calculations.

State	T_v (cm^{-1}) [a]
$X\ ^3\Sigma^-$	0
$1\ ^1\Gamma$	5461
$1\ ^1\Sigma^+$	7318
$1\ ^5\Pi$	5701
$1\ ^3\Delta$	8785
$1\ ^3\Pi$	12 141
$1\ ^3\Phi$	12 129
$1\ ^1\Delta$	17 207
$1\ ^1\Pi$	16 609
$1\ ^1\Phi$	18 780
$1\ ^3H$	19 445
$2\ ^3\Pi$	20 118
$2\ ^3\Phi$	21 977
$3\ ^3\Pi$	22 384
$1\ ^5\Delta$	23 467
$4\ ^3\Pi$	23 632

[a] Vertical term energies calculated at an internuclear distance of 1.69 Å.

Table 8
Ab initio spin-orbit results and tentative assignments to observed transitions.

(Λ, *S*) states[a]	Ω state	E_{SO} (cm^{-1})	Tentative assignment	Observations (using theoretical $a = 1898\ cm^{-1}$)	Observations (using estimated $a = 414\ cm^{-1}$)
$^3\Sigma^-$	0^+	0	$X0^+$		
$^3\Sigma^-$	1	1898	X1[a]		414
$^5\Pi$	0^-	6577	[a+5.4] 0^-	7298	5814
$^5\Pi$	0^+	6679	[a+5.1] 0^+	6998	5514
$^5\Pi$	1	6923	[a+5.6] 1	7498	6014
$^5\Pi$	1	7000	[a+5.9] 1	7798	6314
$^3\Delta/^5\Pi$	3	7115			
$^1\Gamma$	4	7243			
$^5\Pi$	2	7388			
$^3\Delta$	2	10 404			
$^3\Delta/^5\Pi$	3	10 527			
$^1\Sigma^+$	0^+	10 933	[11.0] 0^+	10 965	10 965
$^3\Phi$	2	11 834			
$^3\Pi$	1	12 532			
$^3\Pi$	0^-	13 381			
$^3\Pi$	1	13 771			
$^3\Pi$	0^+	13 904	[a+15.3] 0^+	17 198	15 714
$^3\Phi$	3	14 297			
$^3\Pi$	2	15 322	A′2 ?	17 392 ?	15 908 ?
$^3\Phi$	4	16 896			
$^1\Delta$	2	19 279	A′2 ?	17 392 ?	15 908 ?
$^1\Pi$	1	19 476			
^3H	5	20 586			
$^1\Phi$	3	20 939			
^3H	6	21 580			
$2/3\ ^3\Pi$	0^-	21 614	E′0^- ?	22 170	20 686
$2/3\ ^3\Pi$	0^+	21 638	B′0^+	21 338	19 854
$2/3\ ^3\Pi$	0^-	22 149	E′0^- ?	22 170	20 686
$2/3\ ^3\Pi$	0^+	22 203	E0^+	22 418	22 418
$2\ ^3\Pi$	2	22 224	C′2 ?	21 681	20 197
^3H	7	22 580			
$2\ ^3\Pi$	1	22 758	[a+19.4] 1 ?	21 298	19 814
$2\ ^3\Phi$	2	23 541	[a+20.4] 2 ?	22 298	20 814
$2\ ^3\Phi$	3	24 132			

[a] Strong mixing of (Λ, S) states are indicated by multiple entries.

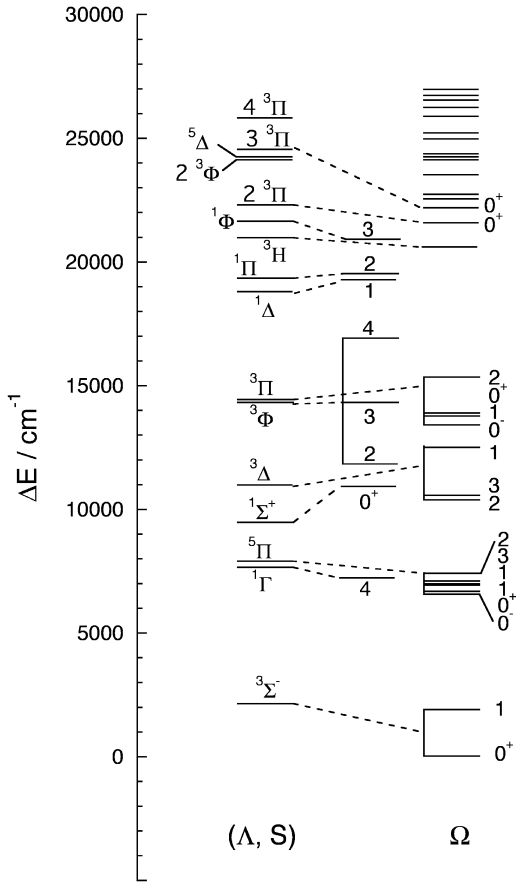

Fig. 9. The splitting from (Λ, S) to Ω states of WO, as calculated by the state interacting method. The correspondence between both levels of theory is indicated by dashed lines for states lying below 22 000 cm^{-1}.

The next calculated excited states are the $^1\Gamma$ and $^3\Delta$ states, but they do not correspond to any of the observed transitions. The $1^1\Sigma^+$ state, calculated at 10 933 cm^{-1}, can be assigned to the [11.0]0$^+$ state observed at 10 965 cm^{-1}. The $1^3\Phi$ and $1^3\Pi$ states exhibit quite large splittings, but the only Ω component of interest is the $1^3\Pi$ 0$^+$ one, calculated at 13 900 cm^{-1}, that could tentatively be assigned to the [15.3]0$^+$ state, in spite of a larger discrepancy than for the lower-lying states. The loss in accuracy can actually be explained by the coupling of the $1^3\Pi$ state with the highly congested region above 20 000 cm^{-1}, where 3 other $^3\Pi$ states interact. The high density of interacting states (see Fig. 9) comes from the high degeneracy of configuration (D) (see Fig. 8). Assignments in this energy range must for this reason be considered as very tentative, as indicated by the question marks in Table 8. However, even if *ab initio* calculations fail to provide explicit assignments, they demonstrate that Ω states corresponding to the higher states (A′, C′, E′, E ...) of the observed transitions exist in this energy window.

There is obviously a remaining problem in current assignment of the low-lying 0$^+$ states because theory predicts that there should be four (from the $X^3\Sigma^-$, $1^1\Sigma^+$, $^5\Pi$ and $1^3\Pi$ states), but six are observed experimentally (X0$^+$, [4.9]0$^+$, [7.5]0$^+$, [11.0]0$^+$, [a+5.1]0$^+$, [a+15.3]0$^+$). As stated earlier, the assignment of the [4.9]0$^+$ state is not completely secure. Since the electronic states of WO tend towards Hund's case (c), the Ω components of the electronic states are widely split and mixed. The electronic assignment of the observed excited states is therefore very challenging.

5. Discussion

The spectroscopic constants for the observed states (Tables 2–4) show that several excited electronic states of group 1 bands are affected by interactions. The excited states of these transitions require higher order effective molecular and Ω-doubling constants to minimize the standard deviations in the fits. This is in fact a reflection of interactions between the excited states. The other unusual feature of the WO bands is the observation of large isotope splittings even in the 0-0 bands of these transitions. For example, the 0-0 bands of the A1–X0$^+$, B1–X0$^+$, C1–X0$^+$, D1–X0$^+$, E0$^+$–X0$^+$ and F0$^+$–X0$^+$ transitions show ^{186}WO–^{184}WO isotope splitting of −0.69, −0.77, −0.26, −0.07, −0.10 cm^{-1}, respectively, which is highly unusual. The vibrational frequencies of these states range from 915 to 985 cm^{-1} while the ground state vibrational frequency is about 1065.6 cm^{-1}, thus predicting a very small but positive ^{186}WO–^{184}WO isotope shift for the 0-0 bands of these transitions. The observation of large and negative shifts means that the heavier species is red shifted. In the cavity ring-down laser absorption study of the F0$^+$–X0$^+$ transition, Kraus et al. [15] resolved the isotopic structure of W^{16}O isotopologues and concluded that the large shift is due to interstate interactions in the excited state. Our analysis of transitions in group 1 supports this conclusion. For example the A1 $v = 0$ (17 165 cm^{-1}) probably interacts with B1 $v = 0$ (17 242 cm^{-1}), B1 $v = 2$ (19 211 cm^{-1}) interacts with C1, $v = 0$ (19 182 cm^{-1}), C1 $v = 2$ (21 032 cm^{-1}) interacts with D1 $v = 0$ (20 794 cm^{-1}) and E0$^+$ $v = 1$ (23 430 cm^{-1}) interacts with F0$^+$ $v = 0$ (23 401 cm^{-1}). From this observation, therefore, we conclude that all of the excited states of group 1, i.e., A1, B1, C1, D1, E0$^+$, and F0$^+$, interact with each other causing anomalous isotope effects. The interactions in the excited state shift the different isotopo-

Table 9
Equilibrium constants[a] (in cm^{-1}) for electronic states of WO.

State	ω_e	$\omega_e x_e$	$\omega_e y_e$	B_e	α_e	γ_e	r_e(Å)
Group1							
F0$^+$	[917.4443(33)]	–	–	0.385337(18)	0.002813(14)	–	1.724218(40)
D1	990.1374(33)	5.5198(13)	0.7036(11)	0.38972(15)	0.00162(18)	–	1.71450(33)
C1	932.5699(54)	2.6613(21)	–	0.394102(25)	0.006111(34)	0.001463(28)	1.704936(54)
B1	988.4476(47)	1.2865(20)	–	0.393745(12)	0.0026954(85)	–	1.705709(23)
A1	927.2141(23)	10.2157(16)	0.7596(21)	0.39495(98)	0.0080(39)	0.99(29)	1.7031(21)
[11.0]	[1023.7031(32)]	–	–	0.4168528(32)	0.0034051(44)	–	1.6577581(64)
[7.5]	[954.3081(50)]	–	–	0.392890(76)	0.001937(11)	–	1.70756(16)
X0$^+$	1065.5951(71)	4.0103(40)	-0.00268(60)	0.4165548(60)	0.0020237(23)	–	1.658351(12)
Group 2							
C′2	[939.5164(26)]	–	–	0.388922(12)	0.001884(17)	–	1.716253(27)
B′0$^+$	[946.7116(24)]	–	–	0.3864354(55)	0.001899(10)	–	1.721766(12)
A′2	[911.5639(46)]	–	–	0.387200(34)	0.001516(32)	–	1.720065(75)
X1	1067.9939(34)	4.0314(16)	–	0.4172526(31)	0.002022(15)	–	1.6569637(62)

[a] Values in square brackets are $\Delta G_{1/2}$ values.

logues by different amounts. Anomalous isotope effects have also been observed in most of the bands of group 2 with the exception of the C′2–X1, 0-0 and D′1-X1, 0-0 bands which show negligible isotope splitting, although the lines are doubled due to Ω doubling.

The spectroscopic constants of Tables 2 and 3 have been used to determine the equilibrium constants for states of groups 1 and 2, which are provided in Table 9. The spectroscopic constants for the $X0^+$ and X1 states are very similar, consistent with their assignment as $X^3\Sigma_{0+}$ and $X^3\Sigma_1$ components of the $X^3\Sigma^-$ ground state. We have not been able to determine the separation between the two components due to the lack of bands connecting them. In our previous paper [17], we estimated a value of 514 cm^{-1} for λ which was found to be incorrect due to an error in the calculation. The revised value for this constant is $\sim$207 cm^{-1} based on our current spectroscopic parameters. The estimated value of the interval between the $X0^+$ and X1 states is, therefore, about 414 cm^{-1} (=2λ).

6. Conclusion

The emission spectrum of WO has been investigated in the 4000–35 000 cm^{-1} interval using a Fourier transform spectrometer. Most of the prominent bands have been rotationally analyzed and classified into three groups. Group 1 consists of nine transitions out of which eight terminate on a common lower state, which has been assigned as $X0^+$ (with $\Omega'' = 0^+$) while the group 2 bands consist of five transitions terminating into a common X1 (with $\Omega'' = 1$) lower state. These two lower states have been assigned as the spin components of the $X^3\Sigma^-$ ground state. This assignment has been supported by our *ab initio* calculations aimed at predicting the spectroscopic properties of the low-lying electronic states of WO. Additional bands consisting of seven transitions (group 3) have been observed in the 9000–15 000 cm^{-1} region. One of these bands observed at 9977 cm^{-1} has it upper state in common with the A′2 state. This observation provides the location of the new states relative to the X1 component and helps in their assignments. Some of the states such as $[a+5.1]0^+$, $[a+5.4]0^-$, [a+5.6]1 and [a+5.9]1, probably involve the spin components of the predicted low-lying $1^5\Pi$ state. An attempt has been made to explain the electronic structure of the other low-lying states of WO based on our experimental results in conjunction with the results of our *ab initio* calculations.

Acknowledgment

We thank M. Dulick of the National Solar Observatory for assistance in obtaining the spectra. The National Solar Observatory is operated by the Association of Universities for Research in Astronomy, Inc., under contract with the National Science Foundation. We thank M. Gerry for pointing out the error in our calculations in reference 17. The research described here was supported by funding from NASA laboratory astrophysics program. Some support was also provided by the UK Engineering and Physical Sciences Research Council (EPSRC). J.L. thanks the Fonds National de la Recherche Scientifique de Belgique (I.I.S.N. project) and the "Communauté française de Belgique–Actions de Recherche Concertées" for financial support.

Appendix A. Supplementary data

Supplementary data for this article are available on ScienceDirect (www.sciencedirect.com) and as part of the Ohio State University Molecular Spectroscopy Archives (http://library.osu.edu/sites/msa/jmsa_hp.htm).

References

[1] F. Gassner, E. Dinjus, W. Leitner, Organometallics 15 (1996) 2078–2082.
[2] M.A. Ciriano, J.J. Parez-Torrente, M.A. Ciriano, L.A. Oro, A. Orejon, C. Claver, Organometallics 18 (1999) 3035–3044.
[3] C.W. Bauschlicher Jr., S.P. Walch, S.R. Langhoff, Quantum chemistry: the challenge of transition metals and coordination chemistry, in: A. Veillard (Ed.), NATO ASI Ser. C, Reidel, Dordrecht, 1986.
[4] A. Gatterer, S.G. Krishnamurthy, Nature 169 (1952) 543.
[5] V. Vittalachar, S.G. Krishnamurthy, Current Sci. (India) 23 (1954) 335–357.
[6] A. Gatterer, J. Junkes, E.V. Salpeter, B. Rosen, Molecular Spectra of Metallic Oxides, Vatican Press, Vatican City, 1957. p. 80.
[7] W. Parkinson, R.W. Nicholls, Unpublished report, 1969.
[8] W. Weltner, D. McLeod, J. Mol. Spectrosc. 17 (1965) 276–299.
[9] D.W. Green, K.M. Ervin, J. Mol. Spectrosc. 89 (1981) 145–158.
[10] A.N. Samoilova, Y.M. Efremov, L.V. Gurvich, J. Mol. Spectrosc. 86 (1981) 1–15.
[11] Y.Y. Kuzyakov, E.N. Moskvitina, E.M. Filippova, Spectrosc. Lett. 30 (1997) 1057–1066.
[12] Y.Y. Kuzyakov, E.N. Moskvitina, E.M. Filippova, Chem. Phys. Reports 17 (1998) 841–849.
[13] M. Lorenz, J. Agreiter, N. Caspary, V.E. Bondybey, Chem. Phys. Lett. 291 (1998) 291–299.
[14] M. Lorenz, V.E. Bondybey, Chem. Phys. 241 (1999) 127–138.
[15] D. Kraus, R.J. Saykally, V.E. Bondybey, Chem. Phys. Lett. 295 (1998) 285–288.
[16] C.J. Nelin, C.W. Bauschlicher, Chem. Phys. Lett. 118 (1985) 221–225.
[17] R.S. Ram, J. Liévin, G. Li, T. Hirao, P.F. Bernath, Chem. Phys. Lett. 343 (2001) 437–445.
[18] S.A. Cooke, C. Krumrey, D.K. Russell, M.C.L. Gerry, Paper #TH04, Presented in the 59th International Symposium on Molecular Spectroscopy (2004).
[19] R.S. Ram, P.F. Bernath, J. Opt, Soc. Am. B 11 (1994) 225–230.
[20] B.A. Palmer, R. Engleman, Atlas of the Thorium Spectrum, Los Alamos National Laboratory, Los Alamos, 1983.
[21] H.-J. Werner, P.J. Knowles, R. Lindh, F.R. Manby, M. Schütz, P. Celani, T. Korona, G. Rauhut, R.D. Amos, A. Bernhardsson, A. Berning, D.L. Cooper, M.J.O. Deegan, A.J. Dobbyn, F. Eckert, C. Hampel, G. Hetzer, A.W. Lloyd, S.J. McNicholas, W. Meyer, M.E. Mura, A. Nicklass, P. Palmieri, R. Pitzer, U. Schumann, H. Stoll, R. Tarroni, T. Thorsteinsson, MOLPRO 2006, version 2006.1.
[22] H.-J. Werner, P.J. Knowles, J. Chem. Phys. 89 (1988) 5803–5914.
[23] P.J. Knowles, H.-J. Werner, Chem. Phys. Lett. 115 (1985) 259–267.
[24] S.R. Langhoff, E.R. Davidson, Int. J. Quantum Chem. 8 (1974) 62.
[25] D. Andrae, U. Häussermann, M. Dolg, H. Stoll, H. Preuss, Theor. Chim. Acta 77 (1990) 123–141.
[26] A. Bergner, M. Dolg, W. Küchle, H. Stoll, H. Preuss, Mol. Phys. 80 (1993) 1431–1441.
[27] R.S. Ram, J. Liévin, P.F. Bernath, J. Mol. Spectrosc. 202 (2000) 116–130.
[28] R.S. Ram, A.G. Adam, W. Sha, A. Tsouli, J. Liévin, P.F. Bernath, J. Chem. Phys. 114 (2001) 3977–3987.
[29] J.M.L. Martin, A. Sundermann, J. Chem. Phys. 114 (2001) 3408–3420.
[30] A. Berning, M. Schweizer, H.-J. Werner, P.J. Knowles, P. Palmieri, Mol. Phys. 98 (2000) 1823–1833.
[31] C. Teichteil, L. Maron, V. Vallet, in P. Schwerdtfeger, editor, "Relativistic electronic structure theory Part 2: Applications", vol. 14 Theoretical and computational chemistry, chapter 8, 476–551, Elsevier Science 2004.